The American Journal of Pathology, Vol. 172, No. 6, June 2008

DOI: 10.2353/ajpath.2008.070829

Neurobiology

Co-Localization of Amyloid Beta and Tau Pathology in Alzheimer's Disease Synaptosomes

Jeffrey A. Fein,[†] Sophie Sokolow,[†] Carol A. Miller,[‖] Harry V. Vinters,[‡¶] Fusheng Yang,[§¶] Gregory M. Cole,[§¶] and Karen Hoppens Gylys*[†]

From the Brain Research Institute, School of Nursing,[†] Department of Pathology and Laboratory Medicine,[‡] and Departments of Medicine[§] and Neurology,[¶] University of California at Los Angeles School of Medicine and Sepulveda Veterans Administration Medical Center and Geriatric Research, Education, and Clinical Care Program, Los Angeles, California; and Departments of Pathology, Neurology, and Program in Neuroscience[‖] Keck University of Southern California School of Medicine, Los Angeles, California*

The amyloid cascade hypothesis proposes that amyloid β (Aβ) pathology precedes and induces tau pathology, but the neuropathological connection between these two lesions has not been demonstrated. We examined the regional distribution and co-localization of Aβ and phosphorylated tau (p-tau) in synaptic terminals of Alzheimer's disease brains. To quantitatively examine large populations of individual synaptic terminals, flow cytometry was used to analyze synaptosomes prepared from cryopreserved Alzheimer's disease tissue. An average 68.4% of synaptic terminals in the Alzheimer's disease cohort (n = 11) were positive for Aβ, and 32.3% were positive for p-tau; Aβ and p-tau fluorescence was lowest in cerebellum. In contrast to synaptic p-tau, which was highest in the entorhinal cortex and hippocampus (P = 0.004), synaptic Aβ fluorescence was significantly lower in the entorhinal cortex and hippocampus relative to neocortical regions (P = 0.0003). Synaptic Aβ and p-tau fluorescence was significantly correlated (r = 0.683, P < 0.004), and dual-labeling experiments demonstrated that 24.1% of Aβ-positive terminals were also positive for p-tau, with the highest fraction of dual labeling (39.3%) in the earliest affected region, the entorhinal cortex. Western blotting experiments show a significant correlation between synaptic Aβ levels measured by flow cytometry and oligomeric Aβ species (P < 0.0001). These results showing overlapping Aβ and tau pathology are consistent with a model in which both synaptic loss and dysfunction are linked to a synaptic amyloid cascade within the synaptic compartment. ***(Am J Pathol 2008, 172:1683–1692; DOI: 10.2353/ajpath.2008.070829)***

Tau pathology is strongly associated with the clinical expression and severity of Alzheimer's disease (AD),[1,2] while early cognitive symptoms correlate with soluble amyloid β (Aβ).[3–6] The importance of the synaptic compartment in disease progression is highlighted by the correlation of early cognitive loss with synapse loss in AD,[7] and by the localization of Aβ42 to multivesicular bodies within pre- and postsynaptic compartments associated with abnormal synaptic morphology.[8,9] The potential importance of synaptic Aβ release is supported by experiments in which lesions of the perforant path reduced amyloid deposition in the hippocampus.

A synaptic Aβ hypothesis is supported by data showing that Aβ42 binding to α7-nicotinic receptors induces N-methyl-D-aspartic acid (NMDA) receptor internalization and impaired glutamatergic transmission.[10] More recently, targeting of oligomer effects to NMDA receptors on dendritic spines have been suggested to promote long-term depression and shrinkage of dendritic spines.[11] Data in triple transgenic mouse models, Down's syndrome, and in human AD tissue suggest that intraneuronal Aβ contributes to early synaptic dysfunction,[12] and a time course study in triple transgenic mice expressing both tau and Aβ mutations suggests that initial Aβ accumulation is intraneuronal and precedes extracellular deposition.[13]

Some controversy surrounds the spatiotemporal mapping of tau and Aβ deposition in AD brains; in general tangle pathology follows a precise anatomical progres-

Supported by grants from the Alzheimer's Association (NIRG-03-6103) and the NIH (5AG016570) (to K.H.G.), the NIH (NS43946) (to G.M.C.), the National Institute on Aging (AG18879) (to C.A.M.), and the NIH (CA 16042 and AI 28697) (to the Jonsson Cancer Center at the University of California at Los Angeles). Tissue was obtained from the Alzheimer's Disease Research Center Neuropathology Cores of the University of Southern California (NIA 050 AG05142) and the University of California at Los Angeles (NIA P50 AG 16570).

Accepted for publication February 27, 2008.

Address reprint requests to Karen H. Gylys, Ph.D., Box 956919 Factor Bldg, Los Angeles, CA 90095-6919. E-mail: kgylys@sonnet.ucla.edu.

sion that is highly correlated with clinical dementia,[14,15] with extracellular amyloid deposition exhibiting a more heterogeneous distribution. The earliest symptoms of AD seem to be associated with neuritic plaques rather than tangles;[16] on the other hand, tangles appear early in the disease process in entorhinal cortex and hippocampus.[1] Like Aβ, altered forms of tau can directly induce caspase-independent cell death and neurotoxicity.[17,18] In animal models, injection of Aβ fibrils has been shown to induce tau pathology,[19] and in triple transgenic mice, intraneuronal oligomers colocalize with somatodendritic tau and anti-oligomer antibodies clear both Aβ and tau pathology. Other links between Aβ and tau pathology include the recent observation that soluble Aβ oligomers (amyloid ß-derived diffusible ligands, ADDLs) induce tau hyperphosphorylation in cultured neurons.[20]

Our recent observation of dense Aβ immunolabeling in synaptic terminals from AD brain and aged Tg2576 mice[21] suggests a connection between intraneuronal Aβ and synaptic dysfunction that is consistent with previous reports of synaptic Aβ release.[22–24] To directly study synaptic changes in AD, we have used flow cytometry quantification of synaptosomal immunolabeling to show marked increases of Aβ in AD cortex and in aged Tg2576 mice, and to show that this synaptic Aβ is accompanied by increased cholesterol, the ganglioside GM1, and synaptosome-associated protein (SNAP)-25.[21] We report here that in fresh AD postmortem tissue, phosphorylated tau (p-tau) accompanies Aβ accumulation in synaptic terminals, and a comparison across seven brain regions shows that synaptic Aβ levels are decreased and p-tau levels are increased in hippocampus and entorhinal cortex compared to neocortical regions.

Materials and Methods

Materials

The monoclonal anti-Aβ antibody 10G4 has been described previously.[25] Polystyrene microsphere size standards were purchased from Polysciences, Inc. (Warrington, PA). Zenon mouse IgG Labeling kits for dual labeling and 4′,6-diamidino-2-phenylindole were purchased from Molecular Probes (Eugene, OR), and rhodamine-conjugated anti-mouse antibody from Chemicon (San Diego, CA). The following monoclonal antibodies were purchased: anti-SNAP-25 (Sternberger Monoclonals Inc., Lutherville, MD), anti-postsynaptic density (PSD) 95 (Upstate Biotechnology, Lake Placid, NY), anti-glial fibrillary acidic protein (GFAP) (Sigma, St. Louis, MO), and AT100 (directed against tau phosphorylated at Ser 212 and Thr214; Pierce, Rockford, IL). The 6E10 antibody was purchased from Signet Labs (Dedham, MA), p422s antibody from Biosource (Camarillo, CA), and the CT20 anti-amyloid precursor protein (APP) antibody from Calbiochem-EMD (Gibbstown, NJ). Filipin was purchased from Sigma-Aldrich (St. Louis, MO).

Human Brain Specimens

Brain samples (frontal [A9], parietal [A39 and A40], superior parietal [A7], hippocampus, entorhinal cortex [A28], and cerebellum) were obtained at autopsy from the Alzheimer's Disease Research Centers at the University of Southern California and the University of California at Los Angeles. Samples were obtained from 11 cases (5 females, 4 males) diagnosed clinically and histopathologically with AD, from two cognitively normal aged controls, and from two neurological control cases with Parkinson's disease only (mean age, 85 years; mean postmortem delay, 5.85 hours).

Crude Synaptosome Preparation

Samples (~0.3 to 5 g), were minced and slowly frozen on the day of autopsy in 10% dimethyl sulfoxide and 0.32 M sucrose and stored at −70°C until homogenization. The crude synaptosome (P-2) fraction was prepared as described previously.[26] Briefly, the homogenate was first centrifuged at 1000 *g* for 10 minutes; the resulting supernatant was centrifuged at 10,000 *g* for 20 minutes to obtain the crude synaptosomal pellet. Aliquots of P-2 are routinely cryopreserved in 0.32 M sucrose and banked at −70°C until the day of the experiment.

Immunolabeling of P-2 Fraction

P-2 aliquots were immunolabeled for flow cytometry analysis according to a method for staining of intracellular antigens.[27] Pellets were fixed in 0.25% buffered paraformaldehyde (1 hour, 4°C) and permeabilized in 0.2% Tween20/PBS (15 minutes, 37°C). Antibodies were labeled directly with Alexa Fluor 488 or 647 reagents according to kit directions. This mixture was added to P-2 aliquots and incubated at room temperature for 30 minutes. Pellets were washed twice with 1 ml 0.2% Tween20/PBS, and then resuspended in PBS buffer (0.75 ml) for flow cytometry analysis. The synaptosomal pellet was dispersed for all washes and for incubations with fixative, detergent, and antibody, and then collected by centrifugation (1310 × *g* at 4°C). For filipin labeling, samples were incubated with a 100 μg/ml solution (20 minutes, room temperature). For cholera toxin labeling, samples were incubated with biotin-conjugated cholera toxin B subunit (10 μg/ml; 25 minutes, room temperature) followed by streptavidin-allophycocyanin (1:200; 25 minutes, room temperature).

Flow Cytometry

Data were acquired using an BD-LSR I analytic flow cytometer (Becton-Dickinson, San Jose, CA) equipped with argon 488 nm, helium-neon 635 nm, and helium-cadmium 325 nm lasers. Five thousand particles were collected and analyzed for each sample. Debris was excluded by establishing a size threshold set on forward light scatter. Alexa 488, Alexa 647, allophycocyanin, and filipin fluorochromes were detected by the FL1, Ssc-W,

Ssc-W, and FL5 photomultiplier tube detectors, respectively. Sorting experiments were performed on a BD FACSAria benchtop, high-speed cell sorter. Analysis was performed using FCS Express software (DeNovo Software, Ontario, Canada).

Confocal Microscopy

Crude P-2 aliquots were immunolabeled as described above and washed, then dispersed with a pipette and spread on slides. Slides were dried, coverslipped with Prolong Antifade (Molecular Probes, Eugene, OR), and stored at 4°C. The Alexa 647 fluor usually used to label SNAP-25 was not compatible with the filter system on the microscope; therefore samples were first incubated with 488-labeled 10G4 antibody and then anti-SNAP-25 antibody (1:1000), followed by secondary antibody (rhodamine-conjugated anti-mouse, 1:200). For human AD brain sections, fresh tissue blocks were postfixed in 4% paraformaldehyde, and snap-frozen in 2-methylbutane (−80°C) before cryostat sectioning. Sections were steamed in retrieval buffer (Vector Laboratories, Burlingame, CA) for 25 minutes before labeling according to the manufacturer's instructions. Confocal fluorescence and differential interference contrast images of synaptosomes and plastic bead standards were taken using a 100×1.4 Planapo objective lens on a Leica TCS-SP Confocal Inverted Microscope (Heidelberg, Germany) equipped with argon (488 nm excitation: blue) and helium-neon (633 nm excitation: red).

Western Blotting

Samples were boiled in Laemmli loading buffer (2%SDS, Invitrogen) and electrophoresed on 10 to 20% Tris-Tricine gradient gels. Gels were stained with Coomasie Blue to ensure equal protein loading. Membranes were blocked for 1 hour at room temperature in 10% nonfat dried milk in PBS, followed by incubation overnight at 4°C with primary antibodies in PBS containing 0.05% Tween 20 (PBS-T) and 1.5% (W/V) albumin. After rinsing in PBS-T, the membranes were incubated with horseradish peroxidase-conjugated anti-mouse IgG (1:10,000) or anti-rabbit IgG (1:30,000) in PBS-T with 1.5% albumin for 1 hour. Immunolabeled proteins were visualized by enhanced chemiluminescence detection reagents. Resulting films were scanned and quantified using densitometric software (Molecular Analyst II, BioRad). To strip immunoblots, membranes were incubated for 30 minutes at 58°C in 100 mmol/L 2-mercaptoethanol, 2% SDS, and 62.5 mmol/L Tris-HCl (pH 6.8). The membranes were rinsed 3–10 minutes in large volumes of PBS-T, followed by re-probing.

Statistics

The within-subjects or repeated measures experimental design used in the present experiments involves multiple measurements on experimental units and has the advantage of reducing error variance resulting from individual differences.[28] For statistical comparisons, the Mixed Procedure in SAS, a generalization of standard linear models used to describe the relationship between multiple variables of interest, was used. A Compound Symmetry covariance structure was used, and custom hypothesis testing for differences between regions used the ESTIMATE statement. Correlation coefficients were calculated with the Pearson product-moment correlation coefficient procedure using the Vassarstat interactive statistical website (*http://faculty.vassar.edu/lowry/VassarStats.html*; Richard Lowry, Poughkeepsie, NY).

Results

Both Aβ and p-tau Accumulate in AD Synaptic Terminals

Neuronal terminals are poorly visualized at the resolution of light microscopy, and immunodetection of Aβ, particularly intraneuronal Aβ, is limited by technical issues that include epitope masking and fixation artifacts.[12] The present experiments used flow cytometry analysis of synaptosomes, which are synaptic terminals that have resealed into a functional sphere during homogenization in isotonic sucrose. Flow cytometry analysis quantifies multiple parameters on each cell or synaptic terminal in a sample; 5000 particles were analyzed for each sample. Fluorescence parameters include both the positive fraction and the brightness of fluorescence, which is expressed as relative fluorescence units. In addition to fluorescence measures, light scattering indicates the size of each particle; forward scatter is proportional to size.

A P-2 (crude synaptosome) fraction was prepared from fresh unfixed AD and control brains with a postmortem interval less than 12 hours; synaptosomal immunolabeling for Aβ, using the 10G4 antibody directed against residues 5 to 17, was quantified by flow cytometry. In support of 10G4 selectivity for Aβ, synaptosomal labeling with 10G4 is blocked by Congo Red,[29] 10G4 strongly labels plaques in AD brain but does not bind APP in immunoprecipitation experiments (not shown), and we have previously shown that monoclonal APP antibodies label a smaller and much less dynamic fraction of synaptic terminals in AD brain.[21] The present experiments confirmed our previous results showing striking increases of synaptic Aβ in AD cortex compared to cognitively normal aged controls (Figure 1, A and B); Aβ labeling in 13-month-old Tg2576 vs. WT mice closely resembles that seen in AD samples (Figure 1, C and D). We have previously demonstrated that non-synaptosomal elements are excluded by drawing a size-based analysis gate that includes only particles that are ~0.75 to 1.5 microns.[29,30] The size standards used to draw the analysis gate are illustrated in Figure 1E. To examine the purity of synaptosomes in the size gate, an experiment was performed in which synaptosomes were physically sorted; in a 9-hour experiment, ~46 million particles were collected based on the size gate. Figure 1 F shows an ultrastructural image of sorted synaptosomes that were placed directly onto a grid and stained with uranyl acetate, revealing spherical synaptosome particles without visible artifacts. The degree of synaptosomal purity in the size-gated anal-

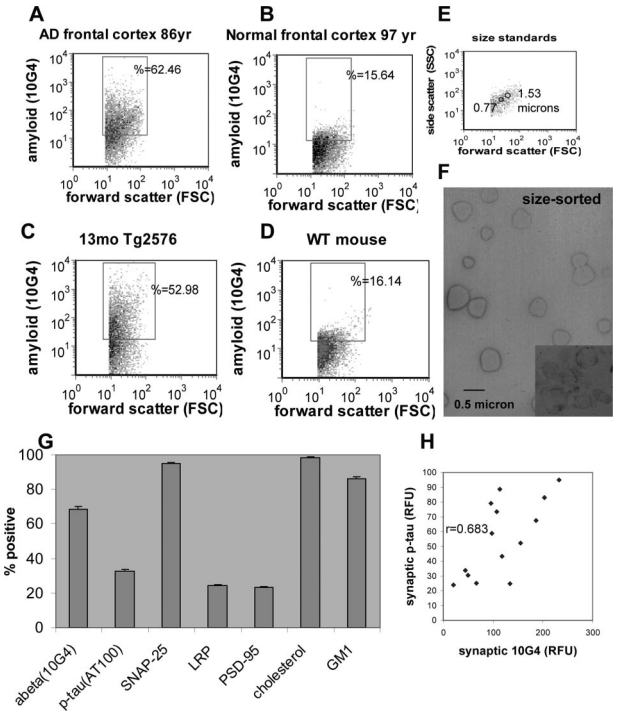

Figure 1. Flow cytometry analysis of Aβ and p-tau in AD synaptosomes. **A–E:** representative samples showing Aβ labeling in synaptosomes from (**A**) AD frontal cortex, (**B**) aged normal frontal cortex, (**C**) aged Tg2576 mouse, and (**D**) wild-type mouse. The forward scatter parameter on the abscissa is proportional to size. **E:** Size standards used to draw the size analysis gate for analysis of particles in the range of ~0.5 to 1.5 microns. **F:** Uranyl acetate-stained electron micrograph image of synaptosomes that were sorted based on the size gate; **inset** from an ultrathin section illustrates internal structure. **G:** Size of positive fraction within the AD cohort for the synaptic and damage markers indicated. Value shown is mean percentage positive across brain regions (A7, A9, A39, A40, A28, and hippocampus, $n = 77$ samples from 11 cases). **H:** Correlation between synaptic Aβ and synaptic p-tau fluorescence (Pearson's product-moment correlation coefficient, $P < 0.004$).

ysis is also indicated by the percentage of that are positive for the docking protein SNAP-25 (95.3%, ± 0.3; Figure 1F); our previous work has shown that SNAP-25 labels a fraction identical in size to synaptophysin and syntaxin.[21]

Figure 1G shows the positive fraction for a number synaptic markers of interest in the cohort of AD cases ($n = 11$; Table 1). The mean number of Aβ-positive synaptosomes, averaged across regions, was 68.4% (±2.0). This compares to 32.3% (±1.6) positive for p-tau using the AT100 antibody, which detects abnormal tau phosphorylation at Ser 212/Thr214. Tau phosphorylation at this epitope has been shown to follow Aβ42 injection in tau transgenic mice[19]; in preliminary studies we have observed similar immunolabeling with the AT8 antibody (not shown). Figure 1G also shows that 24.2% (±0.5) of synaptic terminals are positive for the postsynaptic NMDA scaffold protein PSD-95, and that 95.3% (±0.5) are positive for SNAP-25. Virtually all synaptosomes are also positive for free cholesterol (98.5% ± 0.3), which was assessed by the cholesterol-binding dye filipin. Cholesterol, ganglioside GM1, and low-density lipoprotein receptor-related protein-1 (LRP) have previously been associated with Aβ generation and metabolism, and recent results from our lab showed strong increases in cholesterol and ganglioside GM1 in Aβ-positive synaptosomes.[30] Cholesterol and GM1 are enriched in lipid raft membrane domains, which are hypothesized to be a site of Aβ generation in membranes.[31] GM1 labeled 86.1% (±1.5) and LRP labeled 24.1% (±0.6) of synaptosomes. The mean fluorescence levels measured by flow cytometry for synaptic Aβ and p-tau, taken from Table 1, are significantly correlated ($r = 0.683$, $P < 0.004$; Figure 1H), suggesting an association between Aβ and p-tau pathology in synaptic terminals.

Tissue was obtained from seven brain regions: frontal (A9), parietal (A39 and A40), superior parietal (A7), hippocampus, entorhinal cortex (A28), and cerebellum; the focus of the present study was a comparison of synaptic Aβ and p-tau pathology across a number of brain regions in AD. Therefore a majority of the cases examined (11) were AD cases. Two cognitively normal aged cases and 2 cases with Parkinson's disease were included as comparisons; case details are presented in Table 1, along with the mean fluorescence measured in each case for synaptic terminal Aβ and p-tau, quantified within synaptosomes by flow cytometry. Consistent with previous results,[21] the two cases with Parkinson's disease demonstrated synaptic Aβ levels that were intermediate between the normal aged controls and the AD cases. Interestingly, the dementia case that was neuropathologically determined to have a unique and relatively pure tauopathy (Case 024) displayed relatively low synaptic Aβ and strikingly high synaptic p-tau immunofluorescence, a result that highlights the sensitivity of flow cytometry quantification of synaptic pathology and demonstrates consistency with traditional neuropathology measures. Also of note is the 82-year-old case (Case 735) that did not display clinical dementia but was determined on routine neuropathological examination to have significant changes consistent with a diagnosis of possible AD, Braak stage IV. This case displayed synaptic levels of Aβ and of p-tau that were among the highest measured in the cohort.

Synaptic Aβ Is Decreased and P-Tau Is Increased in Hippocampus and Entorhinal Cortex Compared to the Rest of the Brain

Synaptic Aβ fluorescence was lowest in cerebellum ($P < 0.0001$; Figure 2A). Synaptic Aβ was highest in association neocortex (A7, A9, A39, A40), with intermediate levels measured in hippocampus and entorhinal cortex, which are affected earlier in the disease; the decrease in hippocampus and entorhinal cortex compared to neocortex was statistically significant ($P = 0.0003$). In contrast to synaptic Aβ distribution, p-tau fluorescence was increased in hippocampus and entorhinal cortex compared to neocortical regions ($P = 0.006$, Figure 2B). Figure 2 also shows that cerebellar synaptic terminals are essentially free of p-tau pathology. Synaptic levels of cholesterol and ganglioside GM1 showed similar distributions, with hippocampus and entorhinal cortex significantly higher than neocortical regions (Figure 2C,D; $P < 0.0001$). Relative fluorescence measured for SNAP-25, PSD-95, and LRP did not demonstrate regional variation.

Table 1. Case Information for Synaptosome Samples

No.	Sex	Age (years)	PMI (h)	Braak & Braak score	Frontal cortex atrophy	Neuritic plaques	Neurofib. changes (neuropil threads)	Amyloid fluor. in terminals (RFU)	p-tau fluor in terminals (RFU)
Normals									
726	F	97	5.5	—	Mild	0	0	20.29	23.89
758	M	93	8.5		Mild	Sparse	0	50.1	30.4
PD only									
711	M	74	7.8	PD	Mild	Sparse	Sparse	44.7	33.8
720	M	63	3.5	PD Dementia	Mild	Sparse	Sparse	66.5	25.18
AD cases									
024 *tauopathy*	F	72	5		Prom	0	Marked	58.7	137.3
730 AD def	F	76	3.6	VI	Severe	Sparse	Sparse	96.3	79.0
716 AD def	F	86	5	VI	Severe	Mod	Mod	97.3	58.7
731 AD def	F	87	5.3	V to VI	Mild	Mod	Sparse	107.5	73.3
721 AD def	F	87	5	VI	Mild	Freq	Mod	113.8	88.8
738 AD def+PD	M	83	11	V	Mod	Mod	0	118.1	43.2
752 AD prob	M	98	5.83	III to V	Mod	Mod	0	134.15	24.91
745 AD def	F	92	4.75	V	Mild	Mod	Sparse	155.4	52.13
722 AD poss	M	88	6		Mild	Sparse	Sparse	186.3	67.5
PD + dementia									
735 AD poss no clinical dementia	M	82	4	IV	Mild	Mod	0	203.5	83.1
718 AD def	M	83	7	V	Mild	Freq	Mod	232.8	94.8

Neuropil threads and plaques are reported for frontal cortex and refer to silver (Gallyas) stain. The plaque number includes plaques with and without cores: sparse (<5/field), mod (6 to 20/field), freq (21 to 30/field). RFU, mean relative fluorescence for Aβ and p-tau antibody fluorescence measured by flow cytometry (mean value includes frontal, superior parietal, and parietal (A39 and A40) cortex, hippocampus, entorhinal cortex, and cerebellum).

Synaptic Aβ and P-Tau Are Correlated and Co-Localize within Synaptic Terminals

Because both Aβ and p-tau are present in synaptosomes from AD brain, we next examined for co-localization of Aβ and p-tau within individual synaptic terminals by dual labeling P-2 samples for both Aβ and p-tau followed by flow cytometry analysis; only size-gated particles were analyzed to ensure >90% synaptosomal purity. The degree of co-localization in a representative sample from AD frontal cortex is illustrated in Figure 3A. Only Aβ-positive synaptosomes were acquired and analyzed (5000/sample); particles positive for Aβ only are in the upper left quadrant, and dual positives are in the upper right quadrant. Figure 3B demonstrates that co-localization of Aβ and tau pathology resembling that seen in AD cortex is also observed within synaptic terminals of aged

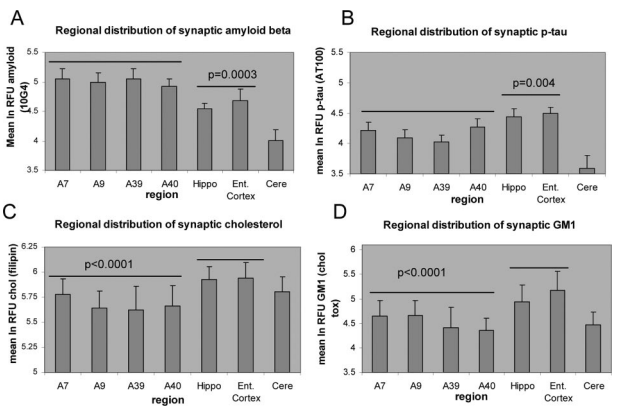

Figure 2. Regional distribution of synaptic (**A**) Aβ, (**B**) p-tau, (**C**) free cholesterol, and (**D**) ganglioside GM1. For each measure, the Estimate statement was used to test for grouped differences between hippocampus and entorhinal cortex versus neocortical regions (A7, A9, A39, and A40).

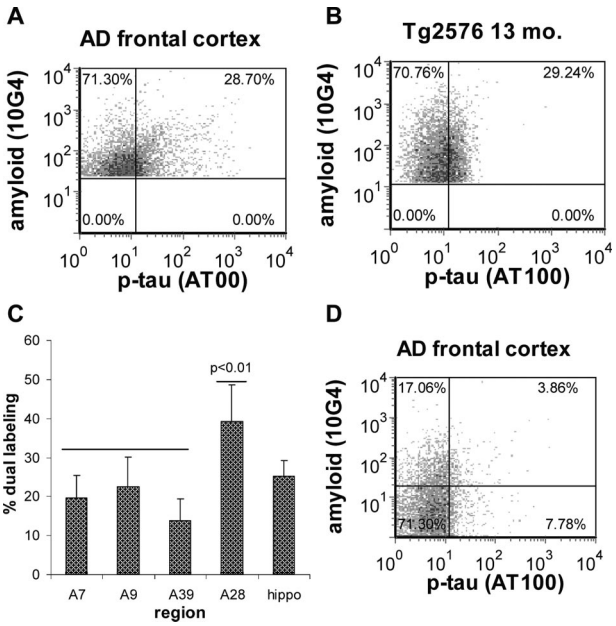

Figure 3. Co-localization of Aβ and p-tau. **A–B:** Flow cytometry quadrant analysis for a representative sample of AD frontal cortex (**A**), and aged Tg2576 mouse (**B**). Only Aβ-positive synaptosomes were analyzed; particles positive for Aβ only are in the upper left quadrant and particles positive for both Aβ and p-tau are in the upper right quadrant, (**C**) regional variation in dual labeled fraction ($n = 29$ samples from 6 cases), (**D**) quadrant analysis of size-gated synaptosomes illustrating size of fraction positive only for p-tau (lower right quadrant).

Tg2576 mice, which overexpress the Swedish mutation of the APP protein and do not express mutated tau. Averaged across regions, 24.1% (±4.3, $n = 35$ samples from six cases) of Aβ-positive terminals were also positive for p-tau. When examined by region, the fraction of dual-labeled particles was significantly higher in entorhinal cortex (39.3%, ±9.3; Figure 3C), compared to superior parietal (19.6%, ±5.8, $P < 0.01$), parietal (13.8%, ±5.6, $P < 0.0001$), and frontal (22.61%, ±7.4, $P < 0.01$) cortex, although the comparison with hippocampus (25.3%, ±4.0) was not significant. To determine the fraction of synaptosomes containing p-tau only, in some experiments 5000 dual labeled synaptosomes were collected within the size gate; particles positive only for tau are in the lower right quadrant, and negatives are in the lower left quadrant. The AD frontal cortex sample in Figure 3D illustrates that a fraction (9.8%, ±7.4, $n = 15$ samples from 3 cases) of synaptosomes is positive for p-tau only, indicating that Aβ may not be requisite within a terminal for tau hyperphosphorylation.

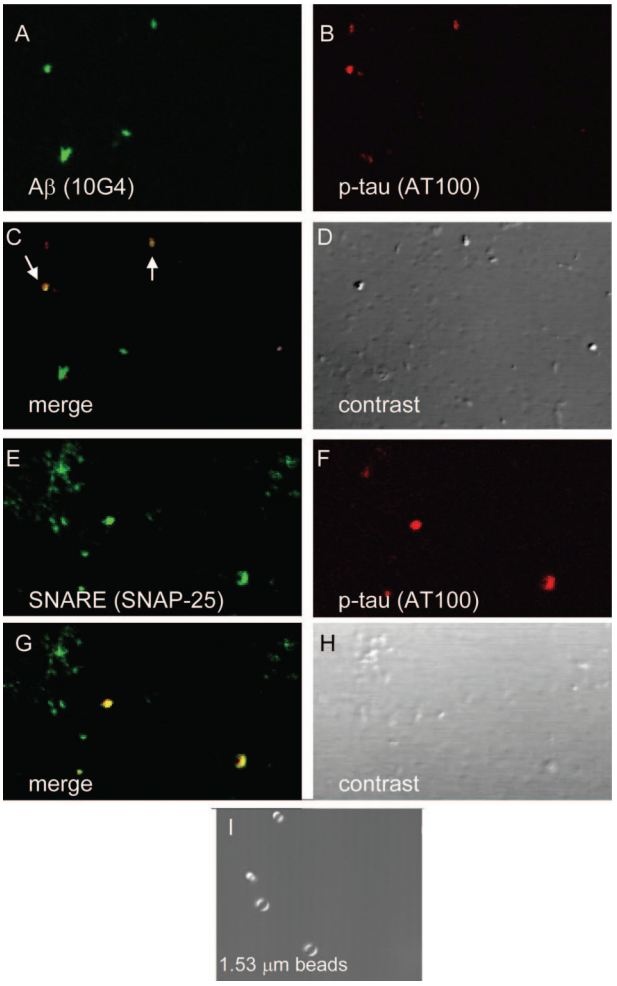

Figure 4. Confocal analysis of Aβ and p-tau co-localization. **A–D:** Confocal analysis of washed P-2 fraction from an 87 y/o AD case (superior parietal cortex) dual labeled for Aβ (A, green) and p-tau (B, red). **C:** Overlay image with yellow color indicating co-localization (**arrows**). **E–H:** Co-localization SNAP-25 (A, green) and p-tau (B, red) indicating co-localization in synaptosomes (**G**). **D, H:** Differential interference contrast images for each field. **I:** 1.53-μm size standards.

Co-localization of Aβ and p-tau within spherical 1 micron particles was confirmed by confocal analysis of P-2 fractions from AD superior parietal cortex (Figure 4). P-2 samples were dual labeled for Aβ (10G4 antibody, green) and p-tau (AT100 antibody, red; Figure 4A, B). The merged image (Figure 4C) shows co-localization of Aβ and p-tau in a subset of synaptosomes; differential contrast images (Figure 4, D and H) reveal the spherical structure and size of the synaptosome particles compared to polystyrene size standards (Figure 4I). The synaptosomal identity of the particles in the washed P-2 fraction is confirmed by dual labeling for p-tau (AT100) and with the SNAP-25 antibody directed against a presynaptic soluble N-ethylmaleimide-sensitive fusion attachment receptor protein (Figure 4E–H).

Correlation of Synaptic Aβ with Oligomeric Aβ Species and Aggregates

Because antigen exposure issues are known to limit visualization of intraneuronal Aβ *in vivo*,[12] and to confirm flow cytometry results, we performed Western analysis of washed P-2 samples from AD cases previously examined by flow cytometry (Table 1). Using the 6E10 antibody (against residues 5 to 10), the immunoblot showed Aβ aggregates and a number of oligomeric species (Figure 5A). An Aβ hexamer species showed a particularly high correlation with the level of synaptic Aβ measured by flow

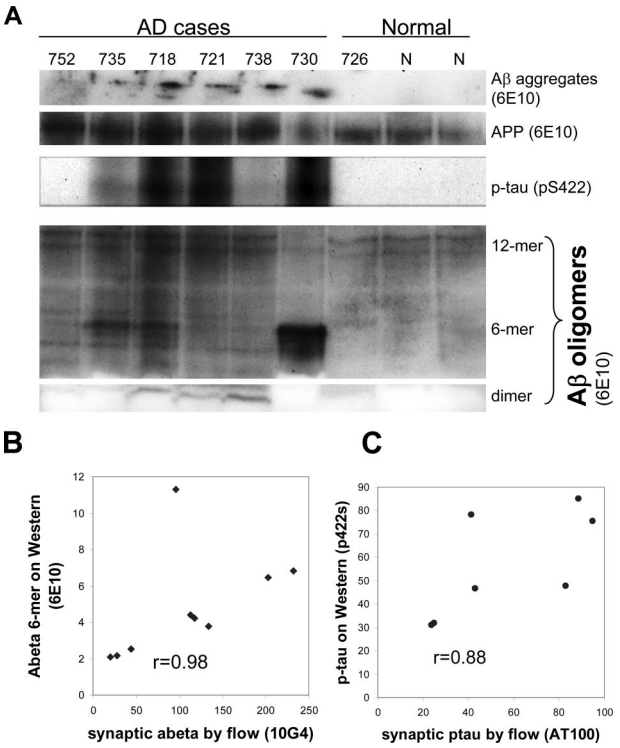

Figure 5. Synaptic Aβ is correlated with oligomers in AD samples. **A:** Western blot of washed P-2 samples from AD cases previously examined by flow cytometry showing multiple Aβ species and APP identified by the 6E10 antibody; p-tau was identified by the p422s antibody. **B:** Correlation of synaptic Aβ measured by flow cytometry (Table 1) with a hexameric oligomer species ($P < 0.0001$ with one outlier removed). **C:** Correlation of synaptic tau measured by flow cytometry with p-tau ($P < 0.0008$).

cytometry with the 10G4 antibody ($r = 0.981$, $P < 0.0001$, with one outlier removed, Figure 5B). Synaptic Aβ also correlated significantly with Aβ dimers ($r = 0.648$, $P < 0.03$), aggregated Aβ in lanes ($r = 0.903$, $P < 0.0005$), and APP ($r = 0.789$, $P < 0.0058$), but did not correlate with beta-site APP cleaving enzyme levels ($r = 0.195$, ns; not shown). Flow cytometry results with the AT100 antibody, which is associated with extracellular tangles and is specific for Alzheimer tau,[32] were confirmed by Western analysis with a polyclonal antibody against p-tau (p422s), an epitope that has been associated with intraneuronal neurofibrillary tangles[33] ($r = 0.88$, $P < 0.0008$; Figure 5C).

Co-Localization of Aβ and P-Tau in Neurites in AD Brain

Confocal imaging of sections from AD hippocampus dual labeled for Aβ (10G4) and p-tau (AT100; Figure 6A–D) revealed abundant p-tau-positive processes that appeared distended. In addition to intense plaque staining, Aβ labeling showed a number of bulbous distal terminals and swollen processes; frequently Aβ labeling was observed in punctuate subcellular structures consistent with previously observed Aβ labeling in multivesticular bodies (Figure 6B).[8,9] Extensive co-localization of Aβ and p-tau was observed in structures that appear to be dystrophic neurites for the N-terminal anti-Aβ antibodies 10G4 and 6E10 (Figure 6, D and E), and the mid-region antibody 4G8 (amino acids 17 to 24, not shown). A C-terminal anti-APP antibody showed diffuse punctuate labeling and intense labeling in globular periplaque dystrophic neurites. In contrast to the anti-Aβ antibodies examined, C-terminal APP labeling does not overlap with AT100-positive neurites (Figure 6F), or with 10G4 (not shown). Co-localization without homogenization in AD brain sections argues against the possibility that synaptic Aβ labeling results from the release of Aβ during the homogenization step required for synaptosome preparation. Also arguing against "sticking" of Aβ to synaptosomes are our experiments showing that Aβ labeling of postmortem AD synaptosomes is not removed by neprilysin or by a combination of trypsin/heparinase (not shown).

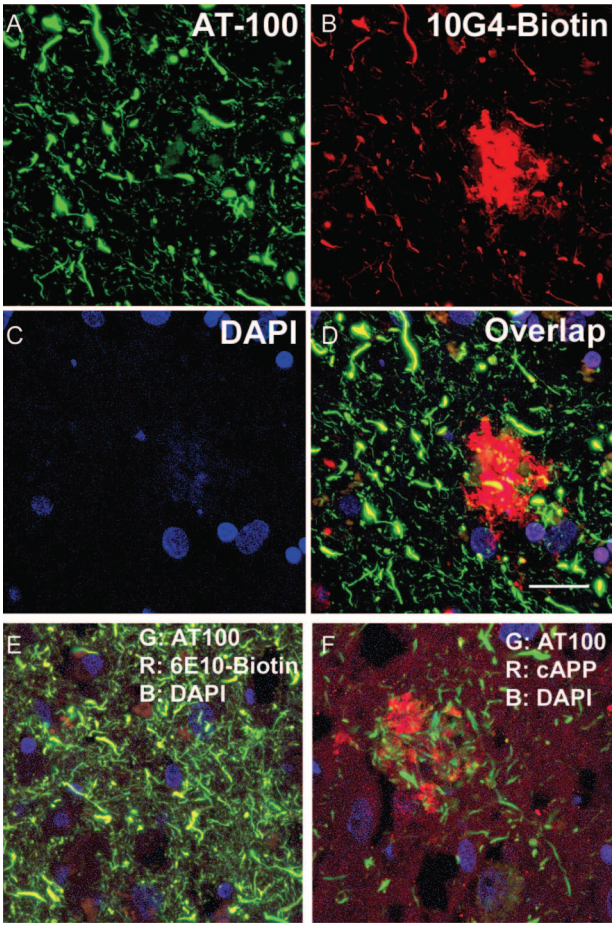

Figure 6. Aβ and p-tau are co-localized in neuronal processes in AD brain. Confocal images of section from AD case showing (**A**) p-tau (green) identified by the AT100 antibody, (**B**) Aβ (red) identified by the 10G4 antibody, and (**C**) nuclei (blue) labeled with 4′,6-diamidino-2-phenylindole. **D:** Overlap shows co-localization (yellow) in multiple dystrophic neurites. **E:** Merged image with 6E10 antibody also shows extensive overlap (yellow) with AT100-positive neurites. **F:** Merged image of C-terminal APP labeling does not show co-localization with p-tau in AT100-positive neurites; Bar = 20 μm.

Discussion

The present experiments use flow cytometry analysis of synaptosomes to demonstrate that AD synaptic terminals contain both Aβ and p-tau. Despite good experimental support in transgenic animal models, the non-overlapping spatial distribution of the two key pathologies in human disease has limited full acceptance of an amyloid cascade hypothesis in which Aβ pathology precedes tau pathology. Co-localization of Aβ and p-tau is highest in the earliest affected regions in AD, and free cholesterol and ganglioside GM1 are also increased in the earliest affected regions. These findings support previous observations of Aβ co-localization with intraneuronal tangles in human cases,[34,35] and with early somatodendritic tau in 3X Tg mice.[36] The present results show overlapping pretangle pathology that localizes to synapses in human disease, and suggest that synaptic loss and dysfunction may be linked to an amyloid cascade within terminals.

Postmortem data are inherently cross-sectional; however, the high degree of co-localization of Aβ and tau pathology in the earliest affected region is consistent with a sequence of events in which amyloid β precedes the appearance of p-tau in synaptic terminals in human disease. This interpretation is consistent with a body of data in 3X Tg mice supporting the initiation of tau pathology by intraneuronal amyloid β accumulation, and is in line with our observation that synaptic p-tau levels are increased in Tg2576 mice, which do not express mutated tau protein.

Our observation of lower Aβ and higher p-tau in medial temporal regions compared to cortex is consistent with the observed predominance of tangles in hippocampus and entorhinal cortex of postmortem cases, while plaques are primarily observed in neocortical areas. However, our working hypothesis has been that synaptic Aβ precedes synapse loss and is a potential seed for Aβ

deposition. Therefore, we anticipated an increase rather than a decrease in Aβ in the earliest affected regions, and the high degree of co-localization in the medial temporal lobe combined with the relatively low level of Aβ fluorescence in these regions was surprising. This result seems most consistent with a scenario in which accumulating Aβ within terminals is released as the disease progresses. A release explanation is in line with recent observations that intraneuronal Aβ decreases with advancing age in transgenic models,[13,37] with increasing age in Down's syndrome,[38] and with increasing cognitive dysfunction and deposition in AD.[39] Synaptic release of Aβ from entorhinal projections to the hippocampus is supported by studies showing that perforant path and entorhinal cortex lesions attenuate hippocampal Aβ deposition,[22,23,40] and by the association of increased interstitial Aβ with synaptic activity *in vivo*.[24] Decreased synaptic Aβ in entorhinal cortex and hippocampus might also result from synapse loss accompanying neuron loss in more affected regions, although in this case one would also expect losses in synaptosomal SNAP-25 and p-tau fluorescence, which are not observed.

Consistent with the long established trans-synaptic spread of pathology from entorhinal cortex and hippocampus to isocortex, in the present experiments we observed a small fraction of synaptosomes positive for p-tau but not Aβ. This indication that tau hyperphosphorylation may not require Aβ accumulation within the same terminal is evidence in human disease for a trans-synaptic mechanism previously demonstrated in mutant tau mice, where injection of Aβ into hippocampus or cortex resulted in remote tangle formation in the amygdala.[19] Alternatively, tau phosphorylation may be induced by highly toxic Aβ oligomers beneath the detection limit of our flow cytometry assay. The dystrophic neurite labeling of Aβ and p-tau in confocal images is not presumed to fully represent the situation in the large populations of smaller (0.5 to 1 micron) synaptosome populations in flow cytometry studies. The periplaque dystrophic neurite labeling likely represents the extreme of a continuum of neuropil labeling that is only resolved by quantitative flow cytometry of single terminals.

In vitro experiments have provided support for a hypothesis that lipid raft microdomains in membranes influence Aβ generation via enhanced access of secretases to APP in the raft environment,[31] and Aβ has been shown to accumulate in lipid rafts in animal models and in AD prefrontal cortex.[41,42] In line with this hypothesis, our previous work has shown strong increases in free cholesterol and GM1 in Aβ positive synaptosomes compared to Aβ-negatives,[29] and the present results show increased synaptic cholesterol and GM1 in the earliest affected regions. GM1 and cholesterol both bind directly to Aβ and have been suggested to initiate fibril formation, so it is also possible that synaptic cholesterol and GM1 contribute to pathological aggregation rather than, or in addition to, generation of Aβ.[43] On the other hand, synaptic Aβ may result from uptake into terminals via raft-mediated binding or through isoform-specific binding of apoE to Aβ followed by LRP-mediated uptake and clearance. Because hippocampus and entorhinal cortex are focal sites for plasticity and receive highly processed inputs from the entire neocortex, the observed increase in synaptic cholesterol and GM1 in the hippocampus and entorhinal cortex may also be associated with a plastic or sprouting response to impaired function in these regions.[44,45]

A synaptic localization for intraneuronal Aβ is in agreement with EM studies showing Aβ localization to multivesicular bodies within presynaptic and postsynaptic compartments.[8] However, diffuse oligomeric deposits also appear pericellularly in AD sections, and exogenously applied oligomers are well documented to target postsynaptic NMDA receptors.[46,47] In addition to triggering intraneuronal damage pathways such as tau-dependent microtubule disassembly,[48] Aβ may be released with synaptic activity[24] or by degenerating neurites; therefore a hypothesis that intracellular Aβ produces cellular and synaptic dysfunction is entirely compatible with evidence that extracellular Aβ also induces dysfunction.

Despite the association of the earliest AD symptoms with plaque pathology,[16] controversy has been generated by the association of clinical progression with tangles rather than plaques, and by the observation that tangles appear before Aβ deposition in entorhinal cortex and hippocampus.[49,50] Many workers in the field have adopted a version of an amyloid cascade hypothesis in which tau pathology mediates the association of Aβ to cognitive decline, a hypothesis with recent support from cases in the Religious Orders study.[51] In animals, reduced tau expression in hAPP mice blocked Aβ-induced cognitive impairments by reducing excitotoxicity,[52] suggesting that tau reduction uncouples Aβ from downstream pathological mechanisms. In primary neurons, tau was required for Aβ-induced microtubule disassembly.[48] Interestingly, tau phosphorylation was not associated with mediation of Aβ effects in the transgenic or culture model, although temporal or spatial constraints may have limited detection of p-tau in these studies.

A possible mechanism involving tau phosphorylation is suggested by the recent observation that intracellular Aβ binds to soluble tau and promotes tau phosphorylation by glycogen synthase kinase-3β; coexpression of Aβ and tau within tangles in postmortem AD sections was also observed.[35] These authors hypothesize that the Aβ-tau complex generates insoluble complexes of both Aβ and tau within neurons, and suggest blockade of Aβ-tau binding may be a viable therapeutic target. Our observation that Aβ and p-tau pathology colocalize within the synaptic compartment in human disease indicates the potential for targeting early Aβ/tau interactions to synaptic terminals, where interventions would be most likely to improve or preserve synaptic function.

Acknowledgments

We acknowledge J. Kotlerman for statistical consultation and O. Ubeda, Q. Ma, M. Cilluffo, and K. Henkins for technical assistance.

References

1. Arriagada PV, Growdon JH, Hedley-Whyte ET, Hyman BT: Neurofibrillary tangles but not senile plaques parallel duration and severity of Alzheimer's disease. Neurology 1992, 42:631–639
2. Bierer LM, Hof PR, Purohit DP, Carlin L, Schmeidler J, Davis KL, Perl DP: Neocortical neurofibrillary tangles correlate with dementia severity in Alzheimer's disease. Arch Neurol 1995, 52:81–88
3. McLean CA, Cherny RA, Fraser FW, Fuller SJ, Smith MJ, Beyreuther K, Bush AI, Masters CL: Soluble pool of Abeta amyloid as a determinant of severity of neurodegeneration in Alzheimer's disease. Ann Neurol 1999, 46:860–866
4. Kuo YM, Emmerling MR, Vigo-Pelfrey C, Kasunic TC, Kirkpatrick JB, Murdoch GH, Ball MJ, Roher AE: Water-soluble Abeta (N-40. N-42) oligomers in normal and Alzheimer disease brains J Biol Chem 1996, 271:4077–4081
5. Naslund J, Haroutunian V, Mohs R, Davis KL, Davies P, Greengard P, Buxbaum JD: Correlation between elevated levels of amyloid beta-peptide in the brain and cognitive decline. JAMA 2000, 283:1571–1577
6. Mucke L, Masliah E, Yu GQ, Mallory M, Rockenstein EM, Tatsuno G, Hu K, Kholodenko D, Johnson-Wood K, McConlogue L: High-level neuronal expression of abeta 1–42 in wild-type human amyloid protein precursor transgenic mice: synaptotoxicity without plaque formation. J Neurosci 2000, 20:4050–4058
7. Terry RD, Masliah E, Salmon DP, Butters N, DeTeresa R, Hill R, Hansen LA, Katzman R: Physical basis of cognitive alterations in Alzheimer's disease: synapse loss is the major correlate of cognitive impairment. Ann Neurol 1991, 30:572–580
8. Takahashi RH, Milner TA, Li F, Nam EE, Edgar MA, Yamaguchi H, Beal MF, Xu H, Greengard P, Gouras GK: Intraneuronal Alzheimer abeta42 accumulates in multivesicular bodies and is associated with synaptic pathology. Am J Pathol 2002, 161:1869–1879
9. Pastorino L, Sun A, Lu PJ, Zhou XZ, Balastik M, Finn G, Wulf G, Lim J, Li SH, Li X, Xia W, Nicholson LK, Lu KP: The prolyl isomerase Pin1 regulates amyloid precursor protein processing and amyloid-[beta] production. Nature 2006, 440:528–534
10. Snyder EM, Nong Y, Almeida CG, Paul S, Moran T, Choi EY, Nairn AC, Salter MW, Lombroso PJ, Gouras GK, Greengard P: Regulation of NMDA receptor trafficking by amyloid-beta. Nat Neurosci 2005, 8:1051–1058
11. Shankar GM, Bloodgood BL, Townsend M, Walsh DM, Selkoe DJ, Sabatini BL: Natural oligomers of the Alzheimer amyloid-beta protein induce reversible synapse loss by modulating an NMDA-type glutamate receptor-dependent signaling pathway. J Neurosci 2007, 27:2866–2875
12. Gouras GK, Almeida CG, and Takahashi RH: Intraneuronal Abeta accumulation and origin of plaques in Alzheimer's disease. Neurobiol Aging 2005, 26:1235–1244
13. Oddo S, Caccamo A, Smith IF, Green KN, LaFerla FM: A dynamic relationship between intracellular and extracellular pools of Abeta. Am J Pathol 2006, 168:184–194
14. Bancher C, Braak H, Fischer P, Jellinger KA: Neuropathological staging of Alzheimer lesions and intellectual status in Alzheimer's and Parkinson's disease patients. Neurosci Lett 1993, 162:179–182
15. Braak H, Braak E, Bohl J: Staging of Alzheimer-related cortical destruction. Eur Neurol 1993, 33:403–408
16. Tiraboschi P, Hansen LA, Thal LJ, Corey-Bloom J: The importance of neuritic plaques and tangles to the development and evolution of AD. Neurology 2004, 62:1984–1989
17. Amadoro G, Ciotti MT, Costanzi M, Cestari V, Calissano P, Canu N: From the cover: nMDA receptor mediates tau-induced neurotoxicity by calpain and ERK/MAPK activation. Proc Natl Acad Sci USA 2006, 103:2892–2897
18. Wang YP, Biernat J, Pickhardt M, Mandelkow E, Mandelkow EM: Stepwise proteolysis liberates tau fragments that nucleate the Alzheimer-like aggregation of full-length tau in a neuronal cell model. Proc Natl Acad Sci USA 2007, 104:10252–10257
19. Gotz J, Chen F, van Dorpe J, Nitsch RM: Formation of neurofibrillary tangles in P301l tau transgenic mice induced by Abeta 42 fibrils. Science 2001, 293:1491–1495
20. De Felice FG, Wu D, Lambert MP, Fernandez SJ, Velasco PT, Lacor PN, Bigio EH, Jerecic J, Acton PJ, Shughrue PJ, Chen-Dodson E, Kinney GG, Klein WL: Alzheimer's disease-type neuronal tau hyperphosphorylation induced by Abeta oligomers. Neurobiol Aging 2007, Mar 31; [Epub ahead of press]
21. Gylys KH, Fein JA, Yang F, Wiley DJ, Miller CA, Cole GM: Synaptic changes in Alzheimer's disease: increased amyloid-beta and gliosis in surviving terminals is accompanied by decreased PSD-95 fluorescence Am J Pathol 2004, 165:1809–1817
22. Lazarov O, Lee M, Peterson DA, Sisodia SS: Evidence that synaptically released beta-amyloid accumulates as extracellular deposits in the hippocampus of transgenic mice. J Neurosci 2002, 22:9785–9793
23. Sheng JG, Price DL, Koliatsos VE: Disruption of corticocortical connections ameliorates amyloid burden in terminal fields in a transgenic model of Abeta amyloidosis. J Neurosci 2002, 22:9794–9799
24. Cirrito JR, Yamada KA, Finn MB, Sloviter RS, Bales KR, May PC, Schoepp DD, Paul SM, Mennerick S, Holtzman DM: Synaptic activity regulates interstitial fluid amyloid-beta levels in vivo. Neuron 2005, 48:913–922
25. Mak K, Yang F, Vinters HV, Frautschy SA, Cole GM: Polyclonals to beta-amyloid(1-42) identify most plaque and vascular deposits in Alzheimer cortex, but not striatum. Brain Res 1994, 667:138–142
26. Gylys KH, Fein JA, Tan AM, Cole GM: Apolipoprotein E enhances uptake of soluble but not aggregated amyloid-beta protein into synaptic terminals. J Neurochem 2003, 84:1442–1451
27. Schmid I, Uittenbogaart CH, Giorgi JV: A gentle fixation and permeabilization method for combined cell surface and intracellular staining with improved precision in DNA quantification. Cytometry 1991, 12:279–285
28. Gliner JA, Morgan GA, Harmon RJ: Single-factor repeated-measures designs: analysis and interpretation. J Am Acad Child Adolesc Psychiatry 2002, 41:1014–1016
29. Gylys KH, Fein JA, Yang F, Miller CA, Cole GM: Increased cholesterol in Abeta-positive nerve terminals from Alzheimer's disease cortex. Neurobiol Aging 2007, 28:8–17
30. Gylys KH, Fein JA, Yang F, Cole GM: Enrichment of presynaptic and postsynaptic markers by size-based gating analysis of synaptosome preparations from rat and human cortex. Cytometry A 2004, 60:90–96
31. Ehehalt R, Keller P, Haass C, Thiele C, Simons K: Amyloidogenic processing of the Alzheimer beta-amyloid precursor protein depends on lipid rafts. J Cell Biol 2003, 160:113–123
32. Zheng-Fischhofer Q, Biernat J, Mandelkow EM, Illenberger S, Godemann R, Mandelkow E: Sequential phosphorylation of Tau by glycogen synthase kinase-3beta and protein kinase A at Thr212 and Ser214 generates the Alzheimer-specific epitope of antibody AT100 and requires a paired-helical-filament-like conformation. Eur J Biochem 1998, 252:542–552
33. Augustinack J, Schneider A, Mandelkow EM, Hyman B: Specific tau phosphorylation sites correlate with severity of neuronal cytopathology in Alzheimer's disease. Acta Neuropathol (Berl) 2002, 103:26–35
34. Grundke-Iqbal I, Iqbal K, George L, Tung YC, Kim KS, Wisniewski HM: Amyloid protein and neurofibrillary tangles coexist in the same neuron in Alzheimer disease. Proc Natl Acad Sci USA 1989, 86:2853–2857
35. Guo JP, Arai T, Miklossy J, McGeer PL: Abeta and tau form soluble complexes that may promote self aggregation of both into the insoluble forms observed in Alzheimer's disease. Proc Natl Acad Sci USA 2006, 103:1953–1958
36. Oddo S, Caccamo A, Tran L, Lambert MP, Glabe CG, Klein WL, LaFerla FM: Temporal profile of amyloid-beta (Abeta) oligomerization in an in vivo model of Alzheimer disease. A link between Abeta and tau pathology. J Biol Chem 2006, 281:1599–1604
37. Wirths O, Multhaup G, Czech C, Feldmann N, Blanchard V, Tremp G, Beyreuther K, Pradier L, Bayer TA: Intraneuronal APP/A beta trafficking and plaque formation in beta-amyloid precursor protein and presenilin-1 transgenic mice. Brain Pathol 2002, 12:275–286
38. Mori C, Spooner ET, Wisniewsk KE, Wisniewski TM, Yamaguch H, Saido TC, Tolan DR, Selkoe DJ, Lemere CA: Intraneuronal Abeta42 accumulation in Down syndrome brain. Amyloid 2002, 9:88–102
39. Gouras GK, Tsai J, Naslund J, Vincent B, Edgar M, Checler F, Greenfield JP, Haroutunian V, Buxbaum JD, Xu H, Greengard P, Relkin NR: Intraneuronal Abeta42 accumulation in human brain. Am J Pathol 2000, 156:15–20
40. Buxbaum JD, Thinakaran G, Koliatsos V, O'Callahan J, Slunt HH, Price DL, Sisodia SS: Alzheimer amyloid protein precursor in the rat hippocampus: transport and processing through the perforant path. J Neurosci 1998, 18:9629–9637
41. Kawarabayashi T, Shoji M, Younkin LH, Wen-Lang L, Dickson DW, Murakami T, Matsubara E, Abe K, Ashe KH, Younkin SG: Dimeric

amyloid beta protein rapidly accumulates in lipid rafts followed by apolipoprotein E and phosphorylated tau accumulation in the Tg2576 mouse model of Alzheimer's disease. J Neurosci 2004, 24:3801–3809
42. Oshima N, Morishima-Kawashima M, Yamaguchi H, Yoshimura M, Sugihara S, Khan K, Games D, Schenk D, Ihara Y: Accumulation of amyloid beta-protein in the low-density membrane domain accurately reflects the extent of beta-amyloid deposition in the brain. Am J Pathol 2001, 158:2209–2218
43. Kakio A, Nishimoto Si, Yanagisawa K, Kozutsumi Y, Matsuzaki K: Cholesterol-dependent formation of GM1 ganglioside-bound amyloid beta-protein, an endogenous seed for Alzheimer amyloid. J Biol Chem 2001, 276:24985–24990
44. Nelson TJ, Alkon DL: Insulin and cholesterol pathways in neuronal function, memory and neurodegeneration. Biochem Soc Trans 2005, 33:1033–1036
45. Dufour F, Liu QY, Gusev P, Alkon D, Atzori M: Cholesterol-enriched diet affects spatial learning and synaptic function in hippocampal synapses. Brain Res 2006, 1103:88–98
46. Lacor PN, Buniel MC, Chang L, Fernandez SJ, Gong Y, Viola KL, Lambert MP, Velasco PT, Bigio EH, Finch CE, Krafft GA, Klein WL: Synaptic targeting by Alzheimer's-related amyloid beta oligomers. J Neurosci 2004, 24:10191–10200
47. Gong Y, Chang L, Viola KL, Lacor PN, Lambert MP, Finch CE, Krafft GA, Klein WL: Alzheimer's disease-affected brain: presence of oligomeric A beta ligands (ADDLs) suggests a molecular basis for reversible memory loss. Proc Natl Acad Sci USA 2003, 100: 10417–10422
48. King ME, Kan HM, Baas PW, Erisir A, Glabe CG, Bloom GS: Tau-dependent microtubule disassembly initiated by prefibrillar beta-amyloid. J Cell Biol 2006, 175:541–546
49. Duyckaerts C: Looking for the link between plaques and tangles. Neurobiol Aging 2004, 25:735–739
50. Schonheit B, Zarski R, Ohm TG: Spatial and temporal relationships between plaques and tangles in Alzheimer-pathology. Neurobiol Aging 2004, 25:697–711
51. Bennett DA, Schneider JA, Wilson RS, Bienias JL, Arnold SE: Neurofibrillary tangles mediate the association of amyloid load with clinical Alzheimer disease and level of cognitive function. Arch Neurol 2004, 61:378–384
52. Roberson ED, Scearce-Levie K, Palop JJ, Yan F, Cheng IH, Wu T, Gerstein H, Yu GQ, Mucke L: Reducing endogenous tau ameliorates amyloid beta-induced deficits in an Alzheimer's disease mouse model. Science 2007, 316:750–754